Structural Monitoring and Maintenance, *Vol. 8, No. 1 (2021) 111-124*
DOI: https://doi.org/10.12989/smm.2021.8.1.111

Continuously inhomogeneous beam structure with creep: a longitudinal crack study

Victor I. Rizov*

Department of Technical Mechanics, University of Architecture, Civil Engineering and Geodesy, 1 Chr. Smirnensky blvd., 1046 – Sofia, Bulgaria

(*Received August 6, 2020, Revised January 6, 2021, Accepted January 8, 2021*)

Abstract. The main purpose of the present paper is to evaluate the influence of increase of the coefficient of viscosity with time on the strain energy release rate for a longitudinal crack in a continuously inhomogeneous beam configuration under linear creep. The beam exhibits continuous material inhomogeneity along the width, thickness and length. The creep behavior is studied analytically by a viscoelastic model structured by one dashpot and three springs. The coefficient of viscosity of the dashpot and the modulii of elasticity of the springs are distributed continuously in the width, thickness and length directions of the beam. Besides, the coefficient of viscosity increases with time. Time-dependent solutions to the strain energy release are derived by considering the balance of the energy and by applying the compliance method. The results obtained by the two solutions are identical which proves the correctness of the analysis performed. The solutions take into account the creep behavior and the increase of the coefficient of viscosity with time. A parametric study of the strain energy release rate is carried-out by using the solutions derived. It is found that the strain energy release rate decreases with increasing of the coefficient of viscosity with time.

Keywords: longitudinal crack; beam structure; viscoelastic behavior; creep; continuous material inhomogeneity

1. Introduction

Continuously inhomogeneous materials are important structural materials which are widely used in various engineering areas such as aerospace, automotive industry, astronautics, nuclear reactors, biomedicine, energy conservation and electronics. The properties of structural members made of these modern materials vary gradually along one or more coordinates. Thus, the material properties are continuous functions of the coordinates. One of the advanced continuously inhomogeneous materials is the functionally graded material. Continuous variations of microstructure and material properties of functionally graded materials are obtained by gradually changing the proportions of the constituent materials along the desired directions in the solid (Avcar and Mohammed 2018, Butcher *et al*. 1999, Çallioglu *et al*. 2011, 2015, Demir *et al*. 2013, Gasik 2010, Han *et al*. 2001, Hedia *et al*. 2014, Hirai and Chen 1999, Nemat-Allal *et al*. 2011, Saiyathibrahim *et al*. 2016, Udupa *et al*. 2014, Sofiyev and Avcar 2010, Sofiyev *et al*. 2012, Uslu

*Corresponding author, Professor, E-mail: V_RIZOV_FHE@UACG.BG

 ISSN: 2288-6605 (Print), 2288-6613 (Online)

Uysal and Kremzer 2015, Uslu Uysal 2015, 2016, Wu *et al*. 2014). Due to the fact that the properties of functionally graded materials can be formed technologically and vary smoothly in the material, these novel composites possess remarkable advantages in comparison with traditional laminated composite. The functionally graded materials find extensive application especially in development of structural members and components subjected to non-uniform exploitation requirements.

In order to design the continuously inhomogeneous (functionally graded) structural members safely, various aspects of the fracture behavior of continuously inhomogeneous materials should be carefully analyzed (Panigrahi and Pohit 2016, Wei *et al*. 2012, Erdogan 1995, Uslu Uysal and Güven 2016, Yang and Chen 2008).

Various problems of linear-elastic fracture mechanics of functionally graded materials have been formulated in Erdogan (1995). The deboning fracture behaviour of functionally graded coatings has been discussed too. The effects of residual and thermal stresses on the fracture have been considered. Delamination cracks in beam structural members with functionally graded surface coatings with linear-elastic behaviour have also been studied.

Functionally graded beam structures with edge cracks have been investigated theoretically assuming linear-elastic behavior of the material (Yang and Chen 2008). The beams under consideration are functionally graded along their thickness only. Cracked beams with different end supports such as clamped-clamped, clamped-free and hinged-hinged have been analyzed.

Fracture analyses of functionally graded beam configurations with axial loading have been developed in (Wei *et al*. 2012). The crack has been modeled by using a rotational spring. Free vibration of cracked beams with linear-elastic mechanical behavior has been studied. The effects of crack location and end supports have been evaluated and discussed. It has been shown that the analyses developed can be used for controlling of damaged functionally graded beams structures.

Fracture behavior of continuously inhomogeneous (functionally graded) beam structures has been studied analytically in Panigrahi and Pohit (2016). Various beam configurations have been analyzed by using the neutral surface as a reference. The material is functionally graded along the beam height. The influence of crack depth on the fracture behavior has been investigated and discussed.

The present paper is focused on analysis of the effect of increase of the coefficient of viscosity with time on the strain energy release rate for a longitudinal vertical crack in a continuously inhomogeneous beam structure that exhibits linear creep behavior. It should be noted that the previous works on longitudinal fracture of continuously inhomogeneous beam configurations do not consider the influence of creep behavior (Rizov 2017, 2018a, b, 2019, 2020, Rizov and Altenbach 2020). However, inhomogeneous materials and structures under long-lasting external loads usually have creep behavior that has to be taken into account in longitudinal fracture analyses. Therefore, developing of analyses with considering of creep is an important problem of fracture mechanics of inhomogeneous structures. Such analyses will contribute for improving of safety, reliability and durability of inhomogeneous structural members subjected to long-lasting loads. It should be mentioned that analysis of longitudinal fracture is an important problem also because continuously inhomogeneous (functionally graded) materials can be built-up layer by layer (Mahamood and Akinlabi 2017, Markworth *et al*, 1995, Miyamoto *et al*. 1999) which is premise for appearance of longitudinal cracks between layers. In the present paper, the time-dependent strain energy release rate is derived by considering the balance of the energy. The results obtained are confirmed by applying the compliance method. The beam under consideration is continuously inhomogeneous along the width, thickness and length. The creep is treated by a

viscoelastic model with one dashpot and three springs (the coefficient of viscosity of the dashpot increases exponentially with time). A parametric study is performed by using the time-dependent solution to the strain energy release rate.

2. Theoretical model. Analysis of the strain energy release rate

A viscoelastic beam configuration is depicted in Fig. 1. The beam has a rectangular cross-section of width, b, and thickness, h. The length of the beam is $2(l_1 + l)$. The beam is subjected to four-point bending by two vertical forces, F, applied at the ends of the beam. A notch of depth, b_1, is cut-out in the lateral surface of the beam as shown in Fig. 1. A longitudinal vertical crack of length, $2a$, is located symmetrically with respect to the mid-span. The cross-sections of the right-hand and left-hand crack arms are rectangles of widths, b_1 and b_2, and thickness, h. The notch divides the right-hand crack arm in two symmetric parts of length, a. It is obvious that the ring-hand crack arm is free of stresses. It should be mentioned that the crack is located in beam portion, D_2D_6, which is loaded in pure bending (Fig. 1).

The beam exhibits linear creep behavior that is described by using the viscoelastic model shown schematically in Fig. 2. The model is structured by one dashpot with coefficient of viscosity, η_{0t}, and three springs with modulii of elasticity, E_a, E_b and E_c. The increase of η_{0t} with time is expressed as

$$\eta_{0t} = \eta_0 e^{\rho t}, \tag{1}$$

where t is time, η_0 is the value of the coefficient of viscosity at $t = 0$, ρ is a material property ($\rho > 0$).

For the viscoelastic model under constant applied stress, $\sigma \rightleftarrows$, it can be written that

$$\sigma = \sigma_\eta + \sigma_b, \tag{2}$$

$$\sigma_a = E_a \varepsilon_a \underset{\rightleftarrows}{,} \tag{3}$$

$$\sigma_b = E_b \varepsilon_b, \tag{4}$$

$$\sigma_\eta = \overset{\rightleftarrows}{\eta}_{0t} \dot{\varepsilon}_\eta \rightleftarrows, \tag{5}$$

$$\sigma_a + \sigma_b = \sigma, \tag{6}$$

$$\underset{\rightleftarrows}{\varepsilon_\eta} + \varepsilon_a = \varepsilon_b, \tag{7}$$

$$\varepsilon_b = \varepsilon, \tag{8}$$

where σ_a, σ_b and σ_η are the stresses in the springs with modulii of elasticity, E_a and E_b, and in the dashpot, respectively. The strains in the springs with modulii of elasticity, E_a and E_b, and in the dashpot are denoted by ε_a, ε_b and ε_η, respectively.

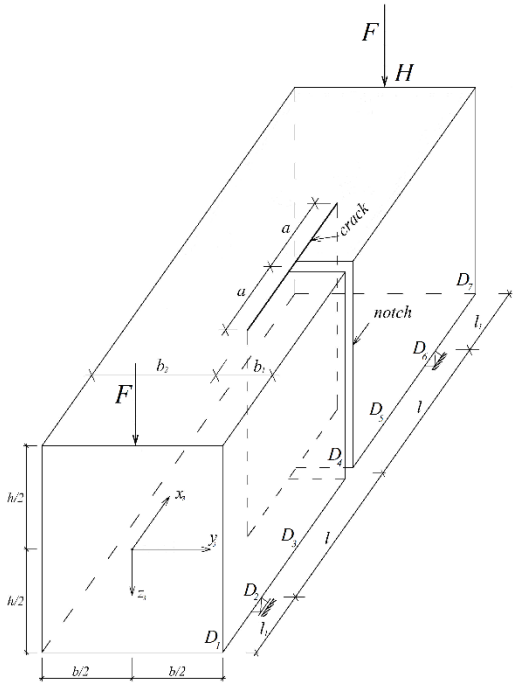

Fig. 1 Geometry and loading of an inhomogeneous viscoelastic beam with a longitudinal crack

By combining of (1)-(8), one obtains

$$\sigma = \eta_0 e^{\rho t}\left[\dot{\varepsilon} - \frac{1}{E_a}\left(\dot{\overset{\rightleftarrows}{\sigma}} - E_b\dot{\overset{\rightleftarrows}{\varepsilon}}\right)\right] + E_b\varepsilon, \tag{9}$$

Since

$$\dot{\overset{\rightleftarrows}{\sigma}} = 0, \tag{10}$$

Eq. (9) takes the form

$$\sigma = \underset{\rightleftarrows}{\eta_0}\, e^{\rho t}\left(\dot{\varepsilon} + \frac{E_b}{E_a}\dot{\varepsilon}\right) + E_b\varepsilon. \tag{11}$$

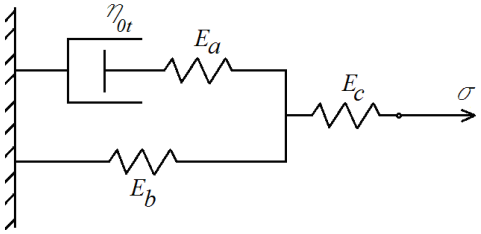

Fig. 2 Linear viscoelastic model with a dashpot and three springs

By solving of (11) with respect to the strain, ε, and adding the strain in the spring with modulus of elasticity, E_c, one obtains the following stress-strain-time relationship for the viscoelastic model shown in Fig. 1

$$\varepsilon = \frac{\sigma}{E_b}\left[1 - e^{\frac{E_b}{Q\rho}(e^{-\rho t}-1)}\right] + \frac{\sigma}{E_a + E_b} e^{\frac{E_b}{Q\rho}(e^{-\rho t}-1)} + \frac{\sigma}{E_c}. \tag{12}$$

where

$$Q_{\rightleftarrows} = \frac{\eta_0(E_a + E_b)}{E_a}. \tag{13}$$

The beam is made of material that is continuously inhomogeneous in width, thickness and length directions. Therefore, the modulii of elasticity and the coefficient of viscosity of the viscoelastic model vary continuously along the width, thickness and length of the beam. The distributions of the modulii of elasticity and the coefficient of viscosity in the beam cross-section are written as

$$E_a = E_{a0} e^{f_{a\rightleftarrows}\frac{\frac{b}{2}+y_3}{b} + g_a \frac{\frac{h}{2}+z_3}{h}}, \tag{14}$$

$$E_b = E_{b0} e^{f_{b\rightleftarrows}\frac{\frac{b}{2}+y_3}{b} + g_b \frac{\frac{h}{2}+z_3}{h}}. \tag{15}$$

$$E_c = E_{c0} e^{f_{c\rightleftarrows}\frac{\frac{b}{2}+y_3}{b} + g_c \frac{\frac{h}{2}+z_3}{h}}, \tag{16}$$

$$\eta = \eta_{0t} e^{f_{\eta\rightleftarrows}\frac{\frac{b}{2}+y_3}{b} + g_{\rightleftarrows\eta} \frac{\frac{h}{2}+z_3}{h}}, \tag{17}$$

where

$$-\frac{b}{2} \le y_3 \le \frac{b}{2}, \tag{18}$$

$$-\frac{h}{2} \le z_3 \le \frac{h}{2}. \tag{19}$$

In formulae (14)-(19), E_{a0}, E_{b0}, E_{c0} and η_{0t} are, respectively, the values of E_a, E_b, E_c and the coefficient of viscosity, $\eta_{\rightleftarrows}$, in the upper left-hand vertex of the beam cross-section, f_a, f_b, f_c, and f_η are, respectively, material properties which control the distributions of E_a, E_b, E_c and $\eta_{\rightleftarrows}$ along the beam width, g_a, g_b, g_c and g_η are, respectively, material properties which control the distributions of E_a, E_b, E_c and $\eta_{\rightleftarrows}$ along the beam thickness, y_3 and z_3 are the centroidal axes of the beam cross-section.

Along the beam length, the distributions of E_{a0}, E_{b0}, E_{c0} and η_0 are expressed as

$$E_{a0} = E_{a0B} e^{s_{a\rightleftarrows}\frac{x_3}{l_1+l}}, \tag{20}$$

$$E_{b0} = E_{b0B} \rightleftarrows e^{s_b \frac{x_3}{l_1+l}}, \tag{21}$$

$$E_{c0} = E_{c0B} e^{s_c \frac{x_3}{l_1+l}}, \tag{22}$$

$$\eta_0 = \eta_{0B} e^{s_\eta \frac{x_3}{l_1+l}}, \tag{23}$$

where

$$0 \leq x_3 \leq l_1 + l. \tag{24}$$

In formulae (20)-(24), E_{a0B}, E_{b0B}, E_{c0B} and η_{0B} are, respectively, the values of E_{a0}, E_{b0}, E_{c0} and η_0 at the ends of the beam, x_3 is the longitudinal centroidal axis of the beam, s_a, s_b, s_c and s_η are material properties controlling the distributions of E_{a0}, E_{b0}, E_{c0} and η_0 along the beam length, respectively. At

$$l_1 + l \leq x_3 \leq 2(l_1 + l), \tag{25}$$

the distributions of E_{a0}, E_{b0}, E_{c0} and η_0 are written as

$$E_{a0} = E_{a0B} e^{s_a \rightleftarrows \frac{2(l_1+l)-x_3}{l_1+l}}, \tag{26}$$

$$E_{b0} = E_{b0B} \rightleftarrows e^{s_b \frac{2(l_1+l)-x_3}{l_1+l}}, \tag{27}$$

$$E_{c0} = E_{c0B} e^{s_c \frac{2(l_1+l)-x_3}{l_1+l}}, \tag{28}$$

$$\eta_0 = \eta_{0B} e^{s_\eta \frac{2(l_1+l)-x_3}{l_1+l}}. \tag{29}$$

Formulae (20)-(29) indicate that the modulii of elasticity and the coefficient of viscosity are distributed symmetrically with respect to the mid-span.

A time-dependent solution to the strain energy release rate for the longitudinal crack in Fig. 1 is derived by considering the balance of the energy. The solution takes into account the linear creep behavior and the increase of the coefficient of viscosity with time. Due to the symmetry, only half of the beam, D_4D_7, is analyzed (Fig. 1). The balance of the energy is written as

$$F\delta w = \frac{\partial U}{\partial a}\delta a + Gh\delta a, \tag{30}$$

where G is the strain energy release rate, w is the vertical displacement of the application point, H, of the external force (Fig. 1), U is the time-dependent strain energy cumulated in half of the beam, δa is a small increase of the crack length.

From (30), one derives

$$G = 2\left(\frac{F}{h}\frac{\partial w}{\partial a} - \frac{1}{h}\frac{\partial U}{\partial a}\right). \tag{33}$$

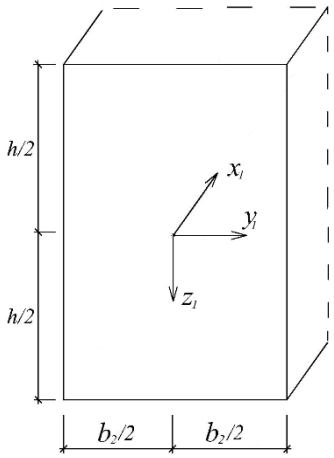

Fig. 3 Cross-section of the left-hand crack arm

The right-hand side of (31) is doubled in view of the symmetry (Fig. 1).

The time-dependent strain energy in half of the beam is written as

$$U = U_1 + U_2, \tag{32}$$

where U_1 and U_2 are the strain energies in portion, D_4D_5, of the left-hand crack arm, and in portion, D_5D_6, of the beam. It should be mentioned that the strain energy cumulated in portion, D_6D_7, of the beam is not involved in (32), respectively in (31) since this strain energy does not depend on the crack length.

The time-dependent strain energy cumulated in portion, D_4D_5, of the left-hand crack arm is found as (Fig. 3)

$$U_1 = \int_0^a \int_{-\frac{b_2}{2}}^{\frac{b_2}{2}} \int_{-\frac{h}{2}}^{\frac{h}{2}} u_{01} dx_1 dy_1 \underset{\rightleftarrows}{} dz_1, \tag{33}$$

where the time-dependent strain energy density, u_{01}, is written as

$$u_{01} = \frac{1}{2}\sigma\varepsilon. \tag{34}$$

By applying the Bernoulli's hypothesis for plane sections, the distribution of strains in the cross-section of the left-hand crack arm is expressed as

$$\varepsilon = \varepsilon_{C_1} + \kappa_{1\rightleftarrows} y_1 + \kappa_2 z_1, \tag{35}$$

where ε_{C_1} is the strain in the centre of the cross-section, κ_1 and κ_2 are the curvatures in the x_1y_1 and x_1z_1 planes, respectively. It should be mentioned that the Bernoulli's hypothesis is applicable since beams of high length to thickness ratio are considered in the present paper.

The following time-dependent equations for equilibrium of the elementary forces in the cross-

section of the left-hand crack arm are used in order to determine ε_{C_1}, κ_1 and κ_2

$$N_1 = \int_{-\frac{b_2}{2}}^{\frac{b_2}{2}} \int_{-\frac{h}{2}}^{\frac{h}{2}} \sigma dy_1 dz_1, \tag{36}$$

$$M_{y_1} = \int_{-\frac{b_2}{2}}^{\frac{b_2}{2}} \int_{-\frac{h}{2}}^{\frac{h}{2}} \sigma z_1 dy_1 dz_1, \tag{37}$$

$$M_{z_1} = \int_{-\frac{b_2}{2}}^{\frac{b_2}{2}} \int_{-\frac{h}{2}}^{\frac{h}{2}} \sigma y_1 dy_1 dz_1, \tag{38}$$

where N_1 is the axial force, M_{y_1} and M_{z_1} are the bending moments with respect to y_1 and z_1. It is obvious that

$$N_1 = 0, \tag{39}$$

$$M_{y_1} = Fl, \tag{40}$$

$$M_{z_1} = 0. \tag{41}$$

By combining of (12) and (35), one obtains

$$\sigma = \left(\underset{\rightleftarrows}{\varepsilon_{C_1}} + \kappa_1 y_1 + \kappa_2 z_1 \right) \left\{ \frac{1}{E_b} \left[1 - e^{\frac{E_b}{Q\rho}(e^{-\rho t}-1)} \right] + \underset{\rightleftarrows}{} \frac{\underset{\rightleftarrows}{\rightleftarrows}\underset{\rightleftarrows}{\rightleftarrows} e^{\frac{E_b}{Q\rho}(e^{-\rho t}-1)}}{E_a + E_b} + \frac{1}{E_c} \right\}^{-1}. \tag{42}$$

After substituting of (42) in (36), (37) and (38), the equations for equilibrium are solved with respect to ε_{C_1}, κ_1 and κ_2 at various values of time by using the MatLab computer program.

The time-dependent strain energy in beam portion, D_5D_6, is written as

$$U_2 = \int_a^l \int_{-\frac{b_{\rightleftarrows}}{2}}^{\frac{b_{\rightleftarrows}}{2}} \int_{-\frac{h}{2}}^{\frac{h}{2}} u_{02} dx_1 dy_{2\,\underset{\rightleftarrows}{}} dz_2, \tag{43}$$

where u_{02} is the time-dependent strain energy density in this beam portion, y_2 and z_2 are the centroidal axes of the cross-section. The strain in the centre of the cross-section and the curvatures of the beam in portion, D_5D_6, are determined by using the equations for equilibrium (36), (37) and (38). For this purpose, b_2 and σ are replaced with b and $\sigma_{D_5D_6}$, respectively. The stress, $\sigma_{D_5D_6}$, in the beam portion, $\sigma_{D_5D_6}$, is expressed by replacing ε_{C_1}, κ_1 and κ_2 with the strain in the centre and curvatures of the beam portion, $\sigma_{D_5D_6}$, in formula (42).

The vertical displacement, w, that is involved in the expression for the time-dependent strain energy release rate (31) is derived by applying the theorem of Castigliano

$$w = \frac{\partial U \underset{\rightleftarrows}{}}{\partial F}. \tag{44}$$

By substituting of (32), (33), (43) and (44) in (31), one derives

$$G = \frac{2}{h}\left[F\frac{\partial}{\partial F}\overrightarrow{\leftarrow}\overrightarrow{\leftarrow}\left(\int_{-\frac{b_2}{2}}^{\frac{b_2}{2}}\int_{-\frac{h}{2}}^{\frac{h}{2}}u_{01}dx_1dy_1\underset{\overrightarrow{\leftarrow}}{}dz_1-\overrightarrow{\leftarrow}\int_{-\frac{b_{\overrightarrow{\leftarrow}}}{2}}^{\frac{b_{\overrightarrow{\leftarrow}}}{2}}\int_{-\frac{h}{2}}^{\frac{h}{2}}u_{02}dx_1dy_2\underset{\overrightarrow{\leftarrow}}{}dz_2\right)\right.$$
$$\left.-\int_{-\frac{b_2}{2}}^{\frac{b_2}{2}}\int_{-\frac{h}{2}}^{\frac{h}{2}}u_{01}dx_1dy_1\underset{\overrightarrow{\leftarrow}}{}dz_1+\overrightarrow{\leftarrow}\int_{-\frac{b_{\overrightarrow{\leftarrow}}}{2}}^{\frac{b_{\overrightarrow{\leftarrow}}}{2}}\int_{-\frac{h}{2}}^{\frac{h}{2}}u_{02}dx_1dy_2\underset{\overrightarrow{\leftarrow}}{}dz_2\right], \tag{45}$$

where the derivative, $\frac{\partial}{\partial F}(\dots)$, is obtained by the MatLab computer program. The integration in (45) is carried-out also by using the MatLab. The time-dependent solution (45) is applied to calculate the strain energy release rate at various values of time.

A time-dependent solution to the strain energy release rate is derived also by using the compliance method. For this purpose, the strain energy release rate is written as

$$G = 2\left(\frac{1}{2h}\overrightarrow{\leftarrow}F^2\frac{dC_{\overrightarrow{\leftarrow}}}{da}\right), \tag{46}$$

where C is the compliance of the beam. The right-hand side of (46) is doubled in view of the symmetry. The compliance is defined as

$$C = \frac{w}{F}, \tag{47}$$

where w is found by using (44).

By combining of (32), (33), (43), (44), (46) and (47), one obtains

$$G = \frac{F}{h}\frac{\partial}{\partial F}\overrightarrow{\leftarrow}\left(\int_{-\frac{b_2}{2}}^{\frac{b_2}{2}}\int_{-\frac{h}{2}}^{\frac{h}{2}}u_{01}dx_1dy_1\underset{\overrightarrow{\leftarrow}}{}dz_1-\overrightarrow{\leftarrow}\int_{-\frac{b_{\overrightarrow{\leftarrow}}}{2}}^{\frac{b_{\overrightarrow{\leftarrow}}}{2}}\int_{-\frac{h}{2}}^{\frac{h}{2}}u_{02}dx_1dy_2\underset{\overrightarrow{\leftarrow}}{}dz_2\right). \tag{48}$$

The integration in (48) is performed by the MatLab computer program. The derivative, $\frac{\partial}{\partial F}(\dots)$, is found also by using the MatLab.

It should be noted that the strain energy release rates obtained by (48) match exactly these calculated by (45). This fact proves the correctness of the time-dependent solutions to the strain energy release rate derived in the present paper.

3. Parametric investigation

The time-dependent solution to the strain energy release rate (45) is applied here in order to carry-out a parametric investigation.

The strain energy release rate is expressed in non-dimensional form by using the formula $G_N = G/(E_{a0B}h)$. The purpose of the parametric investigation is to evaluate the influence of the increasing coefficient of viscosity with time on the strain energy release rate. The influences of the length and location of the longitudinal crack and the material inhomogeneity along the width,

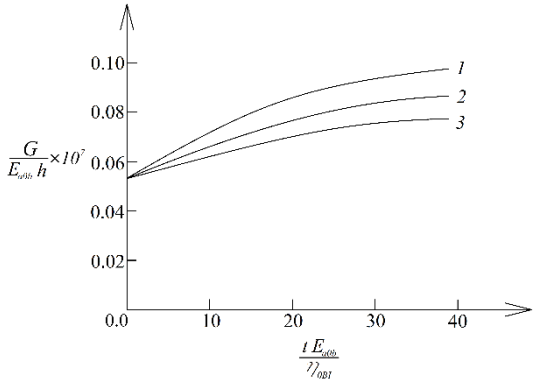

Fig. 4 The strain energy release rate in non-dimensional form presented as a function of non-dimensional time (curve 1 – at $\rho = 0.5$, curve 2 – at $\rho = 1.0$ and curve 3 – at $\rho = 1.5$)

thickness and length of the beam on the strain energy release rate are also evaluated. It is assumed that $b = 0.015$ m, $h = 0.010$ m, $l_1 = 0.020$ m, $l = 0.040$ m and $F = 10$ N.

First, the change of the strain energy release rate with time is evaluated. For this purpose, calculations of the strain energy release rate are carried-out at various values of time.

In order to evaluate the effect of increase of the coefficient of viscosity with time, the strain energy release rate is obtained for three values of ρ. The strain energy release rate in non-dimensional form is presented as a function of non-dimensional time in Fig. 4 for three values of ρ. The time is expressed in non-dimensional form by using the formula $t_N = tE_{a0B}/\eta_{0BI}$. It can be observed in Fig. 4 that the strain energy release rate increases with time (this behavior is due to creep). The curves in Fig. 4 indicate that the strain energy release rate decreases with increasing of ρ. Therefore, it can be concluded that the increase of the coefficient of viscosity with time leads to decrease of the strain energy release rate (physically, this is due to decrease of the deformability).

The influence of material inhomogeneity in the beam cross-section on the strain energy release rate is analyzed too. The findings of this analysis are shown in Fig. 5. First, the influence of the continuous variation of the value of E_a along the width and thickness of the beam cross-section on the strain energy release rate is studied by performing calculations of the strain energy release rate at various values of f_a and g_a. The results of these calculations are illustrated in Fig. 5(a) where the strain energy release rate in non-dimensional form is presented as a function of f_a for three values of g_a. The curves in Fig. 5(a) indicate that the strain energy release rate decreases with increasing of f_a. The increase of material property, g_a, also leads to decrease of the strain energy release rate (Fig. 5(a)). The reason for this behavior is increase of the beam stiffness.

An investigation of the effect of the continuous change of E_b in the width and thickness direction of the beam cross-section is carried-out by calculating the strain energy release rate at various values of f_b and g_b. The results obtained are shown in Fig. 5(b). One can observe in Fig. 5(b) that the strain energy release rate decreases with increasing of f_b and g_b (this is explained by increase of the stiffness).

A similar investigation of the effect of the continuous variation of the value of modulus of elasticity, E_c, along the width and thickness of the cross-section is performed. The calculated strain energy release rate is presented in non-dimensional form as a function of f_c in Fig. 5(c) at three values of g_c. The curves in Fig. 5(c) show that the increase of f_c and g_c leads to decrease of the strain energy release rate.

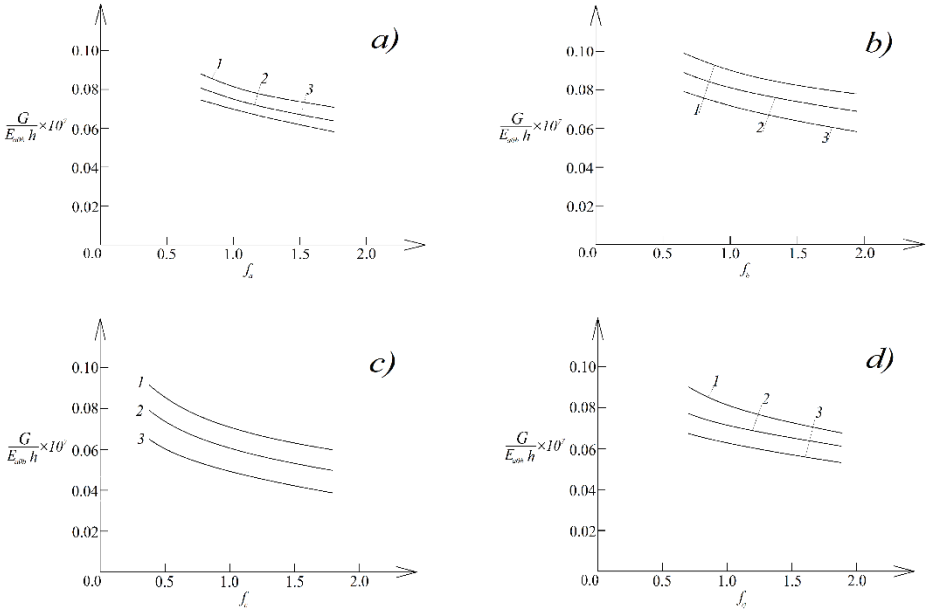

Fig. 5 The strain energy release rate in non-dimensional form presented as a function of (a) f_a (curve 1 – at $g_a = 0.5$, curve 2 – at $g_a = 1.0$ and curve 3 – at $g_a = 2.0$); (b) f_b (curve 1 – at $g_b = 0.5$, curve 2 – at $g_b = 1.0$ and curve 3 – at $g_b = 2.0$); (c) f_c (curve 1 – at $g_c = 0.5$, curve 2 – at $g_c = 1.0$ and curve 3 – at $g_c = 2.0$); (d) f_η (curve 1 – at $g_\eta = 0.5$, curve 2 – at $g_\eta = 1.0$ and curve 3 – at $g_\eta = 2.0$)

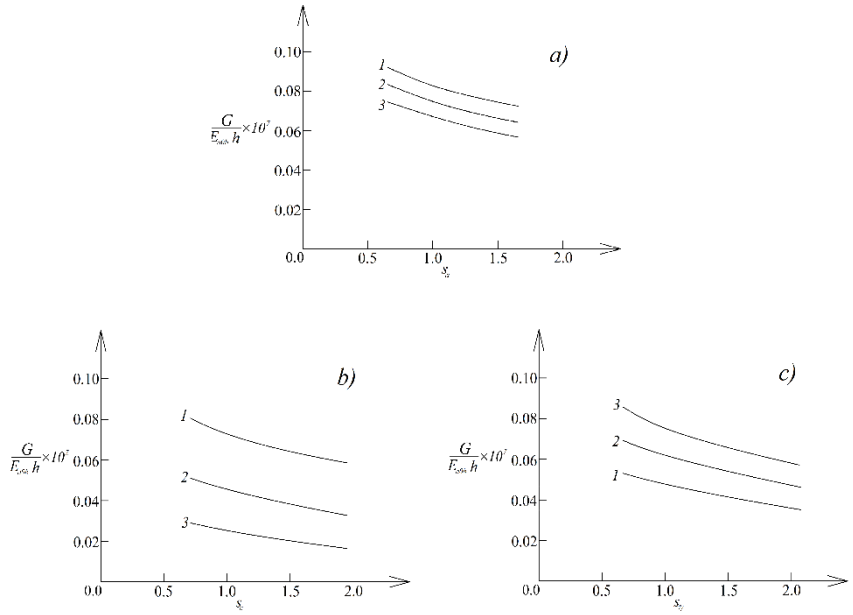

Fig. 6 The strain energy release rate in non-dimensional form presented as a function of (a) s_a (curve 1 – at $s_b = 0.5$, curve 2 – at $s_b = 1.0$ and curve 3 – at $s_b = 2.0$); (b) s_c (curve 1 – at $b_2/b = 0.3$, curve 2 – at $b_2/b = 0.6$ and curve 3 – at $b_2/b = 0.9$); (c) s_η (curve 1 – at $a/l = 0.25$, curve 2 – at $a/l = 0.5$ and curve 3 – at $a/l = 0.75$)

Calculations of the strain energy release rate are carried-out also at various values of f_η and g_η in order to assess the effect of the continuous variation of the coefficient of viscosity along the width and thickness of the beam cross-section. The strain energy release rate in non-dimensional form is presented as a function of f_η at three values of g_η in Fig. 5(d). One can observe in Fig. 5(d) that the strain energy release rate decreases with increasing of f_η and g_η.

The effect of continuous material inhomogeneity along the beam length on the strain energy release rate is also analyzed. The results obtained are shown in graphical form in Fig. 6. First, the effect of continuous variation of the modulii of elasticity, E_a and E_b, along the beam length is studied. For this purpose, calculations of the strain energy release rate are performed at various values of s_a and s_b. One can get an idea for the effect of continuous variation of E_a and E_b along the beam length from Fig. 6(a) where the strain energy release rate in non-dimensional form is presented as a function of s_a at three values of s_b. It can be observed in Fig. 6a that the strain energy release rate decreases with increasing of s_a. The curves in Fig. 6(a) indicate also that increase of s_b leads to decrease of the strain energy release rate. These findings are explained by increase of the stiffness.

The influence of the crack location along the beam width and the continuous variation of the modulus of elasticity, E_c, along the beam length on the strain energy release rate is illustrated in Fig. 6(b) where the strain energy release rate in non-dimensional form is presented as a function of s_c for three values of b_2/b ratio (this ratio characterizes the location of the crack along the beam width). One can observe in Fig. 6(b) that the strain energy release rate decreases with increasing of s_c. Concerning the influence of crack location along the beam width, the curves in Fig. 6(b) show that the strain energy release rate decreases with increasing of b_2/b ratio. This behavior is due to increase of the stiffness of the left-hand crack arm with increasing of b_2/b ratio.

Finally, the influences of the crack length and the continuous variation of the coefficient of viscosity along the beam length on the strain energy release rate are evaluated by performing calculations of the strain energy release rate at various values of a/l ratio and s_η. The strain energy release rate in non-dimensional form is presented as a function of s_η in Fig. 6(c) at three values of a/l ratio. It can be observed that the strain energy release rate decreases with increasing of s_η (Fig. 6(c)). The increase of a/l ratio (this ratio characterizes the crack length) leads to increase of the strain energy release rate (Fig. 6(c)).

4. Conclusions

The strain energy release rate for a longitudinal crack in a continuously inhomogeneous beam configuration under linear creep is analyzed. The creep behavior is described by a linear viscoelastic model structured by one dashpot and three springs. The coefficient of viscosity of the dashpot increases with time. The beam exhibits continuous material inhomogeneity along the width, thickness and length. Therefore, the modulii of elasticity of springs and the coefficient of viscosity vary continuously in the width, thickness and length directions of the beam. Time-dependent solutions to the strain energy release rate that take into account the creep and the increase of viscosity with time are derived by using two approaches (by considering the energy balance and by applying the compliance method). The results yielded by the two approaches are identical. The solutions to the strain energy release rate are applied to perform a parametric study. It is found that the strain energy release rate increases with time (this behavior is due to the creep).

Concerning the effect of the increase of the coefficient of viscosity with time, the study reveals that the strain energy release rate decreases with increase of the coefficient of viscosity. The effects of continuous material inhomogeneity along the width, thickness and length of the beam, the crack length and the crack location along the beam width on the strain energy release rate are also assessed. The calculations indicate that the strain energy release rate decreases with increasing of material properties, f_a, g_a, f_b, g_b, f_c, g_c, f_η, g_η, s_a, s_b, s_c and s_η (these material properties control the variation of the coefficient of viscosity and the modulii of elasticity along the width, thickness and length of the beam). It is found that the strain energy release rate decreases with increasing of b_2/b ratio. The increase of the crack length leads to increase of the strain energy release rate.

References

Avcar, M. and Mohammed, W.K.M. (2018), "Free vibration of functionally graded beams resting on Winkler-Pasternak foundation", *Arab*. *J*. *Geosci*., **11**, 232. http://doi.org/10.1007/s12517-018-3579-2

Butcher, R.J., Rousseau, C.E. and Tippur, H.V. (1999), "A functionally graded particulate composite: Measurements and Failure Analysis", *Acta*. *Mater*., **47**(2), 259-268. https://doi.org/10.1016/S1359-6454(98)00305-X

Çallioglu, H., Sayer, M. and Demir, E. (2011), "Stress analysis of functionally graded discs under mechanical and thermal loads", *Indian J*. *Eng*. *Mater*. *Sci*., **18**(2), 111-118.

Çallioglu, H., Sayer, M. and Demir, E. (2015), "Elastic-plastic stress analysis of rotating functionally graded discs", *Thin-Wall*. *Struct*., **94**, 38-44. https://doi.org/10.1016/j.tws.2015.03.016

Demir, E., Çallioğlu, H. and Sayer, M. (2013), "Free vibration of symmetric FG sandwich Timoshenko beam with simply supported edges", *Indian J*. *Eng*. *Mater*. *Sci*., **20**(6), 515-521.

Erdogan, F. (1995), "Fracture mechanics of functionally graded materials", *Computat*. *Eng*., **5**(1), 753-770. https://doi.org/10.1016/0961-9526(95)00029-M

Gasik, M.M. (2010), "Functionally graded materials: bulk processing techniques", *Int*. *J*. *Mater*. *Product Technol*., **39**(1-2), 20-29. https://doi.org/10.1504/IJMPT.2010.034257

Han, X., Xu, Y.G. and Lam, K.Y. (2001), "Material characterization of functionally graded material by means of elastic waves and a progressive-learning neural network", *Compos*. *Sci*. *Technol*., **61**(10), 1401-1411. https://doi.org/10.1016/S0266-3538(01)00033-1

Hedia, H.S., Aldousari, S.M., Abdellatif, A.K. and Fouda, N.A. (2014), "New design of cemented stem using functionally graded materials (FGM)", *Biomed*. *Mater*. *Eng*., **24**(3), 1575-1588. https://doi.org/10.3233/BME-140962

Hirai, T. and Chen, L. (1999), "Recent and prospective development of functionally graded materials in Japan", *Mater Sci*. *Forum*, **308**(4), 509-514. https://doi.org/10.4028/www.scientific.net/MSF.308-311.509

Mahamood, R.M. and Akinlabi, E.T. (2017), *Functionally Graded Materials*, Springer.

Markworth, A.J., Ramesh, K.S. and Parks, Jr.W.P. (1995), "Review: modeling studies applied to functionally graded materials", *J*. *Mater*. *Sci*., **30**(3), 2183-2193. https://doi.org/10.1007/BF01184560

Miyamoto, Y., Kaysser, W.A., Rabin, B.H., Kawasaki, A. and Ford, R.G. (1999), *Functionally Graded Materials*: *Design*, *Processing and Applications*, Kluwer Academic Publishers, Dordrecht/London/Boston.

Nemat-Allal, M.M., Ata, M.H., Bayoumi, M.R. and Khair-Eldeen, W. (2011), "Powder metallurgical fabrication and microstructural investigations of Aluminum/Steel functionally graded material", *Mater*. *Sci*. *Appl*., **2**(5), 1708-1718. https://doi.org/10.4236/msa.2011.212228

Panigrahi, B. and Pohit, G. (2016), "Nonlinear modelling and dynamic analysis of cracked Timoshenko functionally graded beams based on neutral surface approach", *Proceedings of the Institution of Mechanical Engineers*, *Part C*: *Journal of Mechanical Engineering Science*, **230**(9), 1468-1497.

http://doi.org/10.1177/0954406215576560
Rizov, V.I. (2017), "Analysis of longitudinal cracked two-dimensional functionally graded beams exhibiting material non-linearity", *Frattura ed Integrità Strutturale*, **41**, 498-510. https://doi.org/10.3221/IGF-ESIS.41.61
Rizov, V.I. (2018a), "Non-linear fracture in bi-directional graded shafts in torsion", *Multidiscipl. Model. Mater. Struct.*, **15**(1), 156-169. https://doi.org/10.1108/MMMS-12-2017-0163
Rizov, V.I. (2018b), "Analysis of cylindrical delamination cracks in multilayered functionally graded non-linear elastic circular shafts under combined loads", *Frattura ed Integrità Strutturale*, **46**, 158-17. https://doi.org/10.3221/IGF-ESIS.46.16
Rizov, V.I. (2019), "Influence of material inhomogeneity and non-linear mechanical behavior of the material on delamination in multilayered beams", *Frattura ed Integrità Strutturale*, **47**, 468-481. https://doi.org/10.3221/IGF-ESIS.47.37
Rizov, V.I. (2020), "Longitudinal fracture analysis of inhomogeneous beams with continuously changing radius of cross-section along the beam length", *Strength Fract. Complexity: Int. J.*, **13**, 31-43. https://doi.org/10.3233/SFC-200250
Rizov, V. and Altenbach, H. (2020), "Longitudinal fracture analysis of inhomogeneous beams with continuously varying sizes of the cross-section along the beam length", *Frattura ed Integrità Strutturale*, **53**, 38-50. https://doi.org/10.3221/IGF-ESIS.53.04
Saiyathibrahim, A., Subramaniyan, R. and Dhanapl, P. (2016), "Centrefugally cast functionally graded materials – review", *Proceedings of International Conference on Systems, Science, Control, Communications, Engineering and Technology*, pp. 68-73.
Sofiyev, A.H. and Avcar, M. (2010), "The stability of cylindrical shells containing an FGM layer subjected to axial load on the Pasternak foundation", *Engineering*, **2**, 228-236. https://doi.org/10.4236/eng.2010.24033
Sofiyev, A.H., Alizada, A.N., Akin, Ö. Valiyev, A., Avcar, M. and Adiguzel, S. (2012), "On the stability of FGM shells subjected to combined loads with different edge conditions and resting on elastic foundations", *Acta Mech.*, **223**, 189-204. https://doi.org/10.1007/s00707-011-0548-1
Udupa, G., Rao, S.S. and Gangadharan, K.V. (2014), "Functionally graded composite materials: an overview", *Procedia Mater. Sci.*, **5**(1), 1291-1299. https://doi.org/10.1016/j.mspro.2014.07.442
Uslu Uysal, M. (2015), "Buckling of functional graded polymeric sandwich panel under different load cases", *Compos. Struct.*, **121**, 182-196. https://doi.org/10.1016/j.compstruct.2014.11.012
Uslu Uysal, M. (2016), "Buckling behaviours of functionally graded polymeric thin-walled hemispherical shells", *Steel Compos. Struct., Int. J.*, **21**(1), 849-862. https://doi.org/10.12989/scs.2016.21.4.849
Uslu Uysal, M. and Güven, U. (2016), "A bonded plate having orthotropic inclusion in the adhesive layer under in-plane shear loading", *J. Adhes.*, **92**, 214-235. https://doi.org/10.1080/00218464.2015.1019064
Uslu Uysal, M. and Kremzer, M. (2015), "Buckling behaviour of short cylindrical functionally gradient polymeric materials", *Acta Physica Polonica*, **A127**, 1355-1357. https://doi.org/10.12693/APhysPolA.127.1355
Wei, D., Liu, Y. and Xiang, Z. (2012), "An analytical method for free vibration analysis of functionally graded beams with edge cracks", *J. Sound Vib.*, **331**(7), 1686-1700. https://doi.org/10.1016/j.jsv.2011.11.020
Wu, X.L., Jiang, P., Chen, L., Zhang, J.F., Yuan, F.P. and Zhu, Y.T. (2014), "Synergetic strengthening by gradient structure", *Mater. Res. Lett.*, **2**(1), 185-191. https://doi.org/10.1080/21663831.2014.935821
Yang, J. and Chen, Y. (2008), "Free vibration and buckling analyses of functionally graded beams with edge cracks", *Compos. Struct.*, **83**(1), 48-60. https://doi.org/10.1016/j.compstruct.2007.03.006